The Astrophysical Journal Letters, 904:L28 (4pp), 2020 December 1 https://doi.org/10.3847/2041-8213/abc958

Specific Effect of Peculiar Velocities on Dark-energy Constraints from Type Ia Supernovae

Dragan Huterer[1,2,3]
[1] Department of Physics, University of Michigan, 450 Church Street, Ann Arbor, MI 48109-1040, USA
[2] Leinweber Center for Theoretical Physics, University of Michigan, 450 Church Street, Ann Arbor, MI 48109-1040, USA
[3] Max-Planck-Institut für Astrophysik, Karl-Schwarzschild-Str. 1, D-85748 Garching, Germany
Received 2020 October 16; revised 2020 November 9; accepted 2020 November 9; published 2020 December 2

Abstract

Peculiar velocities of Type Ia supernova (SN Ia) host galaxies affect the dark-energy parameter constraints in a small but very specific way: the parameters are biased in a single direction in parameter space that is a priori knowable for a given SN Ia data set. We demonstrate the latter fact with a combination of inference from a cosmological *N*-body simulation with overwhelming statistics applied to the Pantheon SN Ia data set, then confirm it by simple quantitative arguments. We quantify small modifications to the current analyses that would ensure that the effect of cosmological parameters is essentially guaranteed to be negligible.

Unified Astronomy Thesaurus concepts: Type Ia supernovae (1728); Galaxy radial velocities (616); Dark energy (351)

1. Introduction

Peculiar velocities complicate the Hubble diagram of Type Ia supernovae (SN Ia). An SN Ia host galaxy with the peculiar velocity $\boldsymbol{v}$ will affect the observed apparent magnitude of the supernova, shifting the observed redshift to $(1 + z_{\rm obs}) = (1 + z)(1 + v_\parallel/c)$ (e.g., Huterer et al. 2015), where z and $z_{\rm obs}$ are the true and observed redshift, and $v_\parallel$ is the peculiar velocity projected along the line of sight. It is often convenient to recast the shift in SN Ia redshifts to that on the SN Ia magnitudes; the latter is (assuming hereafter that $v_\parallel/c \ll 1$ and $z \ll 1$)

$$\delta m \simeq \frac{5}{\ln 10}\frac{(1+z)^2}{H(z)d_L(z)}\frac{v_\parallel}{c}, \qquad (1)$$

where d_L is its luminosity distance, $H(z)$ is the Hubble parameter, and $v_\parallel$ is the component of peculiar velocity parallel to the line of sight. For an SN Ia at $z \simeq 0.01$ and peculiar velocities of order $v_\parallel \simeq 150$ km s^{-1}, this is a shift of $\delta m \simeq (5/\ln 10)(v_\parallel/cz) \simeq 0.1$ mag, though rapidly decreases with increasing SN Ia distance.

The effect of peculiar velocities on cosmological inferences from SN Ia has long been recognized, as it would shift the inferred cosmological parameters, notably the matter and dark-energy densities relative to critical, Ω_M and Ω_Λ, and the dark-energy equation of state parameter w (e.g., Cooray & Caldwell 2006; Hui & Greene 2006; Davis et al. 2011). To ameliorate the effect of peculiar velocities on cosmology, early papers advocated adding a peculiar-velocity dispersion of $\simeq$(300–400) km s^{-1} to the magnitude error (Riess et al. 1998, 2004; Perlmutter et al. 1999; Astier et al. 2006; Wood-Vasey et al. 2007; Kowalski et al. 2008; Kessler et al. 2009; Sullivan et al. 2011), in addition to cutting out the lowest-redshift ($z \lesssim 0.015$) supernovae from the analysis. A more principled and effective approach is to explicitly model the covariance of SN Ia due to peculiar velocities (Gorski 1988; Sugiura et al. 1999; Bonvin et al. 2006; Cooray & Caldwell 2006; Hui & Greene 2006), thus adding such a "signal" covariance to the "noise" contribution from a combination of statistical and observational systematic errors. The covariance-matrix approach has been pioneered in the SN Ia analysis by Conley et al. (2011), and has been adopted, with some variation in the implementation, in most subsequent analyses (Davis et al. 2011; Betoule et al. 2014; Scolnic et al. 2014; Jones et al. 2018; Brout et al. 2019). Most of the recent SN Ia analyses additionally attempt to remove the effect of peculiar velocities by using measurements (e.g., Hudson et al. 2004; Lavaux & Hudson 2011) from velocity-reconstructed maps of the nearby large-scale structures.

Previous work has found that, once the triple-pronged measures of removing the lowest-redshift objects, correcting the nearby supernovae for bulk flows, and modeling the full velocity covariance are enacted, peculiar velocities do not appreciably affect dark-energy inferences from SN Ia (e.g., Davis et al. 2011; Scolnic et al. 2014). Nevertheless, this has occasionally been called into question, often based on suspicions about a possible large "bulk flow" that may lead to larger-than-expected peculiar-velocity effects (Mohayaee et al. 2020). While overwhelming evidence shows that dark-energy constraints of SN Ia are not fundamentally changed by peculiar velocities (Rubin & Hayden 2016; Rubin & Heitlauf 2020) and that SN Ia alone indicate that the velocity field is in agreement with Λ cold dark matter (ΛCDM) expectations (Feindt et al. 2013), it is possible that a smaller effect of peculiar velocities on dark-energy constraints remains.

In this work we calculate, for the first time to our knowledge, the effect of peculiar velocities on dark-energy constraints evaluated directly from a numerical "*N*-body" simulation. This approach is robust against any assumptions about isotropy of either the SN Ia distribution or peculiar-velocity field, and explicitly circumvents any assumptions about the quality of the velocity-field reconstruction. The only assumption is that the dark-matter halo velocities trace that of SN Ia host galaxy velocities—that is, that the velocity bias is equal to unity; this is expected to hold to an excellent accuracy for our purposes (Wu et al. 2013; Armitage et al. 2018). To be maximally conservative, we add the full effect of simulation-inferred peculiar velocities on the current SN Ia data but neglecting any peculiar-velocity corrections that could be made. Incorporating

the latter, as is the practice in contemporary SN Ia analyses, would further ameliorate the effect of peculiar velocities presented in this work, though to an extent that has not yet been quantified in detail. We now describe our procedure in detail.

2. Methodology

2.1. Fiducial SN Ia Data and Cosmological Models

We adopt the Pantheon set of 1048 SN Ia covering the redshift range $0.01 < z < 2.26$ (Scolnic et al. 2018). We use the full covariance of SN Ia magnitude measurements,[4] which consists of both noise and signal. In order to test the sensitivity of our results to the way the covariance has been implemented, we have experimented with removing the off-diagonals in the published Pantheon covariance, then adding back corresponding values from our own calculation (specifically, Equation (3.2) in Huterer et al. 2017). We find that the results are robust with respect to such variations. Of course, ignoring the velocity covariance altogether would lead to larger effects of peculiar velocities; we emphasize that all of our results refer to the case when the SN Ia covariance has been fully implemented.

We consider two cosmological models: (1) the curved ΛCDM model defined with energy densities of matter and dark energy, Ω_M and Ω_Λ (as well as the nuisance Hubble-diagram shift parameter $\mathcal{M}$), and (2) the flat wCDM model defined by Ω_M (where $\Omega_\Lambda = 1 - \Omega_M$), constant equation of state of dark energy w, and $\mathcal{M}$. We compute the fiducial constraints using `CosmoMC` (Lewis & Bridle 2002). The fiducial constraints, with errors quoted around the mean, are $\Omega_M = 0.319 \pm 0.071$, $\Omega_\Lambda = 0.73 \pm 0.11$ (curved ΛCDM), and $\Omega_M = 0.339 \pm 0.064$, $w = -1.24 \pm 0.24$ (flat wCDM).

2.2. Peculiar Velocities from N-body Simulation

To measure and incorporate the effect of peculiar velocities from an N-body simulation, we repeat a very similar procedure to that in Wu & Huterer (2017). We place an observer at different locations in a large simulation, identify the closest-matching halos to actual SN Ia host galaxy locations in the Pantheon sample, and directly calculate the effect of peculiar velocities on cosmological inferences.

Specifically, we use the public release of the Dark Sky simulations[5] (Skillman et al. 2014), which is run using the adaptive tree code `2HOT` (Warren 2013). The cosmological parameters correspond to a flat ΛCDM model and are consistent with Planck and other probes (e.g., Planck Collaboration XIII 2016): $\Omega_M = 0.295$; $\Omega_b = 0.0468$; $\Omega_\Lambda = 0.705$; $h = 0.688$; $\sigma_8 = 0.835$. The dark-matter halos are identified using the halo finder `Rockstar` (Behroozi et al. 2013), and we adopt the largest volume `ds14_a` with $10240^3 = 1.07 \times 10^{12}$ particles within $(8\,h^{-1}\,\mathrm{Gpc})^3$.

We then divide this $(8\,h^{-1}\,\mathrm{Gpc})^3$ volume into 512 subvolumes of $(1\,h^{-1}\,\mathrm{Gpc})^3$, and consider halos with virial mass $M_{\rm vir} \in [10^{12.3}, 10^{12.4}]\,M_\odot$ (which is roughly the Milky Way mass). In each subvolume, we first identify the halo that is closest to the center; this will be the location of that subvolume's observer. Relative to this observer location, we then find the closest halo to each Pantheon SN Ia location in space (a halo in our mass range can be typically find within $\sim 15\,h^{-1}$ Mpc of a given 3D location).

While the relative positions of SN Ia in redshift and angle are fixed, the orientation of their coordinate system relative to that of the simulation frame is arbitrary and, given the highly inhomogeneous distribution of SN in the volume, may likely lead to additional variance. To account for this, we explore all possible orientations of the SN Ia frame relative to the (fixed) subvolume frame. To vary over the orientations, we employ 3240 Euler angles; see the Appendix of Wu & Huterer (2017) for details. We therefore have a sample of 512×3240, or around 1.65 million, realizations of peculiar-velocity field centered at an observer. In each realization, the radial velocity of SN Ia is given simply by

$$v_{\parallel,i} \equiv \boldsymbol{v}_i \cdot \frac{(\boldsymbol{r}_i - \boldsymbol{r}_{\rm obs})}{|\boldsymbol{r}_i - \boldsymbol{r}_{\rm obs}|}, \tag{2}$$

where $\boldsymbol{r}_i$ and $\boldsymbol{v}_i$ are the location and velocity of the closest halo to the ith SN Ia, and $\boldsymbol{r}_{\rm obs}$ is the location of the observer. We add this peculiar velocity to Pantheon SN Ia magnitudes at[6] $z < 0.1$ by employing Equation (1). We then calculate the cosmological biases as described in the next subsection.

Because we are looking at the relative *change* in the effective redshift of observed SN Ia, we assume that the measured $v_{\rm pec}$ of their host halos has been unaccounted for and is to be added to the (cosmic microwave background rest-frame) redshift measured in Pantheon objects. As mentioned in the introduction, this assumption is clearly conservative, as it assumes that the misestimate of the peculiar velocity is large, being equal to its full value of $v_{\rm pec}$ for each SN Ia (the expected error is presumably some fraction of the measured $v_{\rm pec}$).

2.3. Cosmological-parameter Bias Calculation

We finally need to calculate the biases in the cosmological parameters given peculiar-velocity shifts in SN Ia magnitudes. To do that, we adopt the Fisher matrix bias formula (Knox et al. 1998; Huterer 2002) and calculate the linearized shift in the cosmological parameters $\{p_i\}$ given the change in the redshifts due to peculiar velocities:

$$\delta p_i \approx (F^{-1})_{ij} \sum_{a,b} \delta(m)_a\, \boldsymbol{C}\,[m(z_a), m(z_b)]^{-1}\, \frac{\partial \bar{m}(z_b)}{\partial p_j}, \tag{3}$$

where δm is the magnitude shift due to peculiar velocity given in Equation (1), $\boldsymbol{C}$ is the full SN Ia data covariance, and $\partial \bar{m}(z_b)/\partial p_j$ is the sensitivity of the theoretically computed magnitude to shifts in cosmological parameters. Finally, F is the Fisher matrix (approximation of the inverse parameter covariance matrix) for the distribution of SN Ia in Pantheon and the three cosmological parameters that are, recall, $(\Omega_M, \Omega_\Lambda, \mathcal{M})$ and $(\Omega_M, w, \mathcal{M})$, respectively, for the two models that we study. The Fisher bias formula is expected to be accurate in the limit of small shifts, which is what we have at hand. We explicitly tested its accuracy by recomputing the full cosmological constraints for the case when SN Ia magnitudes are shifted by peculiar velocities in a few numerical realizations, and verified that the final shifts in the best-fit values in the parameters $\{p_i\}$ are accurately approximated by Equation (3). Finally, for each peculiar-velocity realization, we evaluate $\Delta\chi^2_{\rm 2d} = (\boldsymbol{\delta p})^T \boldsymbol{F}^{-1}_{\rm 2x2} (\boldsymbol{\delta p})$, where $\boldsymbol{\delta p}$ is the length-two

[4] https://github.com/dscolnic/Pantheon
[5] http://darksky.slac.stanford.edu
[6] We do this to speed up calculations, and have checked that the results are completely converged for this redshift range.

Table 1
Summary of the Statistics of Shifts in the (Projected) Two-dimensional Dark-energy-parameter Plane of Interest

	Cosmological-parameter Biases					
	Curved (Ω_M, Ω_Λ) Model			Flat (Ω_M, w) Model		
$z_{\rm min}$ ($N_{\rm SN}$)	Median $\Delta\chi^2_{\rm 2d}$	$p(\Delta\chi^2_{\rm 2d} > 2.3)$	Relative FoM	Median $\Delta\chi^2_{\rm 2d}$	$p(\Delta\chi^2_{\rm 2d} > 2.3)$	Relative FoM
0.01 (1048)	0.38	9.7%	1.0	0.48	14.2%	1.0
0.02 (1002)	0.30	5.8%	0.99	0.37	8.7%	0.95
0.03 (953)	0.14	0.55%	0.94	0.17	1.25%	0.89

Note. We show the median shift in χ^2, the percentage of realizations that have $\Delta\chi^2$ greater than 2.3 (the Gaussian 68% value), and the relative figure-of-merit (inverse area of the 2D contour) in the given parameter plane.

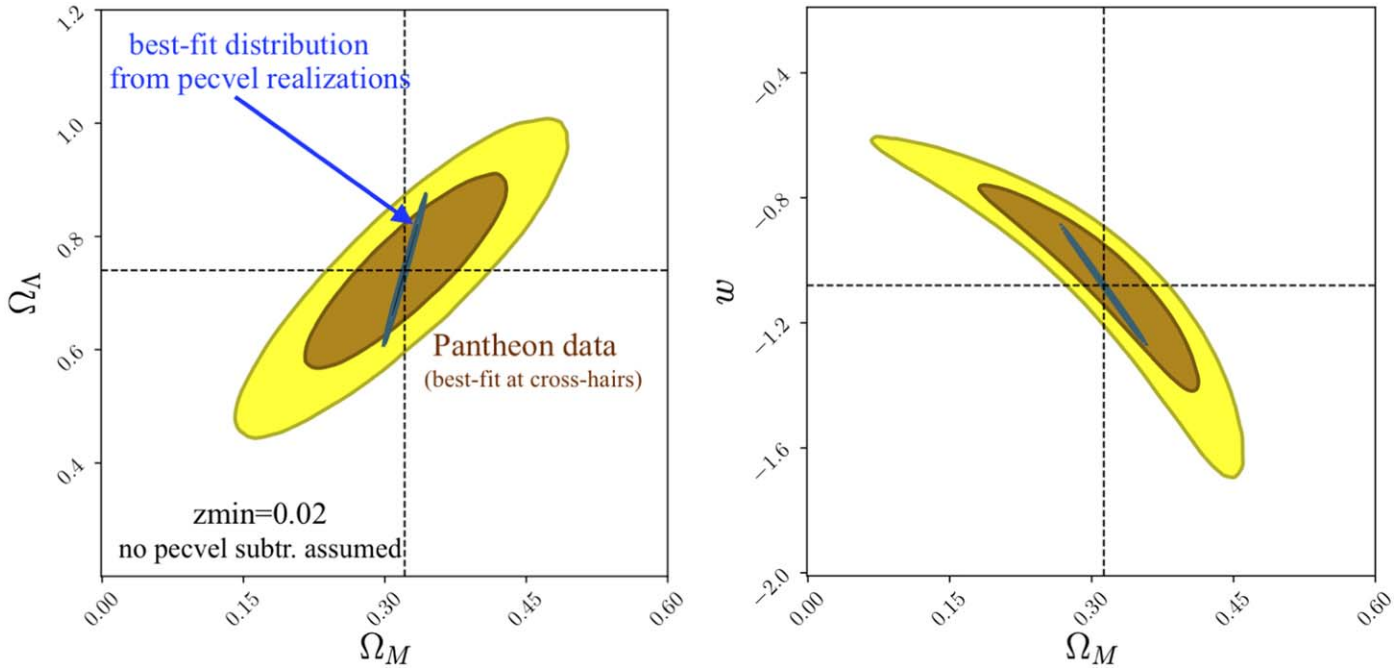

Figure 1. Yellow contours show the fiducial 68.3% and 95.4% C.L. constraints on (Ω_M, Ω_Λ) (left panel) and (Ω_M, w) (right panel) with the fiducial Pantheon SN Ia data set. The blue contours show the 68.3% and 95.4% intervals of the shifts of the best-fit model (whose central value—the mean from our chains—is shown by the crosshairs), evaluated from 1.65 million realizations of the peculiar-velocity field. In this plot we use SN Ia with $z > 0.02$. See the text for other details.

vector of biases in the two parameters, and $\boldsymbol{F}_{\rm 2x2}$ is the Fisher matrix projected to the relevant two-dimensional parameter space.

3. Results

We perform the analysis described above for three cases of the minimum redshift of SN Ia: $z_{\rm min} = 0.01$ (which contains all 1048 Pantheon SN Ia), $z_{\rm min} = 0.02$ (1002 SN Ia), and $z_{\rm min} = 0.03$ (953 SN Ia). As $z_{\rm min}$ increases, the statistical results slightly weaken, but the peculiar-velocity-induced biases dramatically decrease. We wish to study the interplay between the two effects, with the desired goal to keep as many of the low-z objects as possible (Linder 2006).

The results are shown in Table 1. For each of the three $z_{\rm min}$ choices, and for both (Ω_M, Ω_Λ) and (Ω_M, w) parameter space, we show the median $\Delta\chi^2_{\rm 2d}$, the percentage of realizations that have $\Delta\chi^2_{\rm 2d}$ greater than 2.3 (the Gaussian 68% value), and the relative figure-of-merit (F0M; inverse area of the relevant 2D contour). We observe that the biases (quantified by $\Delta\chi^2_{\rm 2d}$) start out nonnegligible, but dramatically decrease with $z_{\rm min}$, while the FoM decreases very slightly from $z_{\rm min} = 0.01$ to 0.02, and somewhat more but still modestly from 0.02 to 0.03.

The results for both models and for $z_{\rm min} = 0.02$ are pictorially shown in Figure 1. The fiducial 68.3% and 95.4% constraints from Pantheon are given with the two larger set of contours, with the best-fit (mean value from the chains) given in the crosshairs. The smaller set of contours in each panel describes the distribution of shifts of the best-fit value in cosmological parameters due to peculiar velocities. Recall that there are 1.65 million such realizations; they are distributed with mean very close to zero (so that the *mean* peculiar-velocity realization does not affect the fiducial Pantheon analysis), and spread described by two contours that describe the 68.3% and 95.4% mass of the parameter shifts.

Moreover, Figure 1 dramatically illustrates that the contours have a very specific direction in either 2D plane. The direction is given by

$$\begin{aligned} \delta\Omega_\Lambda &= +5.7\,\delta\Omega_M \qquad (\text{curved } \Omega_M - \Omega_\Lambda) \\ \delta w &= -4.3\,\delta\Omega_M \qquad (\text{flat } \Omega_M - w), \end{aligned} \tag{4}$$

where the coefficients vary slightly as a function of $z_{\rm min}$; the above values are for $z_{\rm min} = 0.02$. Inspection of Figure 1 shows

that the one-dimensional approximation to the general biased in the respective 2D spaces is entirely appropriate.

The fact that the cosmological-parameter biases always lie in (fixed) 1D directions hints at the fact that the SN Ia Hubble diagram is mainly sensitive to the overall monopole of the peculiar-velocity field—the overall sky-averaged gradient centered at the observer. We explicitly checked this by calculating the biases in cosmological parameters by artificially shifting the SN Ia Hubble diagram at low z ($z \lesssim 0.03$) by an arbitrary but redshift-independent amount δm and repeating the parameter-bias calculation using Equation (3). The resulting bias agrees well with Equation (4) and blue contours in Figure 1, confirming that the bias is driven by the overall divergence of the density field evaluated at the observer's location (the "monopole").

The remaining task is to ensure that the peculiar-velocity effects are negligible. To that end, we employ the simplest strategy of simply adjusting the minimal redshift in order to suppress the bias while ensuring a healthy population of low-z SN Ia that are required to have excellent cosmological constraints. Results in Table 1 indicate that $z_{\rm min} = 0.02$ is sufficient to protect against biases. Perhaps a more realistic estimate of the biases in current SN Ia analyses is obtained assuming that *half* of the peculiar velocities are removed by the velocity-field-correction techniques. In that case, and for $z_{\rm min} = 0.02$, the fraction of cases when $\chi^2_{\rm 2d} > 2.3$ reduces to mere 0.07% and 0.02% for the two respective cosmological models.

4. Discussion and Conclusions

We have evaluated the effect of (uncorrected-for) peculiar velocities on the cosmological constraints from the Pantheon SN Ia data set. Our inference is based on a large-volume N-body simulation with more than 1.5 million realizations of the local peculiar-velocity field. Given these overwhelming statistics, we are confident that our procedure accurately reflects the ensemble of peculiar-velocity fields allowed within ΛCDM, and that any purported cases of a "local void" are captured within the statistical distribution. The two assumptions we have made are (1) that the cosmological model is the current ΛCDM (which is at least approximately true given excellent constraints from non-SN Ia data), and (2) that the velocity bias—velocities of galaxies relative to those of dark-matter halos—is close to unity, which is also supported by independent work.

We find that the peculiar velocities bias the cosmological parameters in very specific 1D directions; see Figure 1. This, in turn, indicates that the dominant effect of peculiar velocities is their overall monopole relative to the observer. We back up this conjecture with a simple numerical experiment.

No subtraction of peculiar velocities was assumed in our procedure. Therefore, the results shown in Table 1 and Figure 1 represent a conservative estimate of the effects of peculiar velocities. They indicate that, even under these conservative assumptions, removing $z \lesssim 0.02$ SN Ia, along with the "good-health habit" of including the full velocity covariance, leads to negligible biases in the cosmological parameters.

We thank Heidi Wu for earlier collaboration on Wu & Huterer (2017), and Alex Kim, Eric Linder, and Fabian Schmidt for useful feedback on the manuscript. D.H. is supported by DOE, NASA, NSF, and Alexander von Humboldt Foundation. We analyzed the Markov Chain Monte Carlo chains and plotted their results using `ChainConsumer` (Hinton 2016).

ORCID iDs

Dragan Huterer https://orcid.org/0000-0001-6558-0112

References

Armitage, T. J., Barnes, D. J., Kay, S. T., et al. 2018, MNRAS, 474, 3746
Astier, P., Guy, J., Regnault, N., et al. 2006, A&A, 447, 31
Behroozi, P. S., Wechsler, R. H., & Wu, H.-Y. 2013, ApJ, 762, 109
Betoule, M., Kessler, R., Guy, J., et al. 2014, A&A, 568, A22
Bonvin, C., Durrer, R., & Gasparini, M. A. 2006, PhRvD, 73, 023523
Brout, D., Scolnic, D., Kessler, R., et al. 2019, ApJ, 874, 150
Conley, A., Guy, J., Sullivan, M., et al. 2011, ApJS, 192, 1
Cooray, A., & Caldwell, R. R. 2006, PhRvD, 73, 103002
Davis, T. M., Hui, L., Frieman, J. A., et al. 2011, ApJ, 741, 67
Feindt, U., Kerschhaggl, M., Kowalski, M., et al. 2013, A&A, 560, A90
Gorski, K. 1988, ApJL, 332, L7
Hinton, S. R. 2016, JOSS, 1, 00045
Hudson, M. J., Smith, R. J., Lucey, J. R., & Branchini, E. 2004, MNRAS, 352, 61
Hui, L., & Greene, P. B. 2006, PhRvD, 73, 123526
Huterer, D. 2002, PhRvD, 65, 063001
Huterer, D., Shafer, D. L., & Schmidt, F. 2015, JCAP, 2015, 033
Huterer, D., Shafer, D. L., Scolnic, D. M., & Schmidt, F. 2017, JCAP, 2017, 015
Jones, D. O., Scolnic, D. M., Riess, A. G., et al. 2018, ApJ, 857, 51
Kessler, R., Becker, A. C., Cinabro, D., et al. 2009, ApJS, 185, 32
Knox, L., Scoccimarro, R., & Dodelson, S. 1998, PhRvL, 81, 2004
Kowalski, M., Rubin, D., Aldering, G., et al. 2008, ApJ, 686, 749
Lavaux, G., & Hudson, M. J. 2011, MNRAS, 416, 2840
Lewis, A., & Bridle, S. 2002, PhRvD, 66, 103511
Linder, E. V. 2006, PhRvD, 74, 103518
Mohayaee, R., Rameez, M., & Sarkar, S. 2020, arXiv:2003.10420
Perlmutter, S., Aldering, G., Goldhaber, G., et al. 1999, ApJ, 517, 565
Planck Collaboration XIII 2016, A&A, 594, A13
Riess, A. G., Filippenko, A. V., Challis, P., et al. 1998, AJ, 116, 1009
Riess, A. G., Strolger, L.-G., Tonry, J., et al. 2004, ApJ, 607, 665
Rubin, D., & Hayden, B. 2016, ApJL, 833, L30
Rubin, D., & Heitlauf, J. 2020, ApJ, 894, 68
Scolnic, D., Rest, A., Riess, A., et al. 2014, ApJ, 795, 45
Scolnic, D. M., Jones, D. O., Rest, A., et al. 2018, ApJ, 859, 101
Skillman, S. W., Warren, M. S., Turk, M. J., et al. 2014, arXiv:1407.2600
Sugiura, N., Sugiyama, N., & Sasaki, M. 1999, PThPh, 101, 903
Sullivan, M., Guy, J., Conley, A., et al. 2011, ApJ, 737, 102
Warren, M. S. 2013, arXiv:1310.4502
Wood-Vasey, W. M., Miknaitis, G., Stubbs, C. W., et al. 2007, ApJ, 666, 694
Wu, H.-Y., Hahn, O., Evrard, A. E., Wechsler, R. H., & Dolag, K. 2013, MNRAS, 436, 460
Wu, H.-Y., & Huterer, D. 2017, MNRAS, 471, 4946